ESTIMATION OF THE ADMITTANCE MATRIX IN POWER SYSTEMS UNDER LAPLACIAN AND PHYSICAL CONSTRAINTS

Morad Halihal and Tirza Routtenberg

School of Electrical and Computer Engineering
Ben-Gurion University of the Negev

ABSTRACT

Admittance matrix estimation in power networks enables faster control actions following emergency scenarios, energy-saving, and other economic and security advantages. In this paper, our goal is to estimate the network admittance matrix, i.e. to learn connectivity and edge weights in the graph representation, under physical and Laplacian constraints. We use the nonlinear AC power flow measurement model, which is based on Kirchhoff's and Ohm's laws, with power and voltage phasor measurements. In order to recover the *complex-valued* admittance matrix, we formulate the associated constrained maximum likelihood (CML) estimator as the solution of a constrained optimization problem with Laplacian and sparsity constraints. We develop an efficient solution using the associated alternating direction method of multipliers (ADMM) algorithm with an ℓ_1 relaxation. The ADMM algorithm is shown to outperform existing methods in the task of recovering the IEEE 14-bus test case.

***Index Terms*—** Admittance matrix estimation, power system topology, graph learning, topology identification, alternating direction method of multipliers (ADMM)

I. INTRODUCTION

The modern electric grid is one of the largest and most complex cyber-physical systems today. Topology information is a critical component of modern Energy Management Systems (EMSs) for multiple monitoring purposes, including analysis, security, control, and stability assessment of power systems [1], [2]. In particular, grid optimization and monitoring tasks entail gaining knowledge of grid topology (connectivity) and line parameters, which are summarized in the admittance matrix of the network. An additional use for topology identification (aka admittance matrix estimation) is event detection, such as identifying faults and line outages [3], [4]. Moreover, it can be used to secure the system from cyberattacks and to determine its potential vulnerabilities [5], [6]. The importance of admittance matrix estimation has increased with the penetration of renewable energy resources.

Different approaches have been suggested for learning the topology of electrical networks. Detecting topological changes in power systems and identifying edge disconnections in general networks were studied in [7], [8] and [4], respectively. The methods in [9]–[12], however, can only reveal part of the grid information, such as the grid connectivity and the eigenvectors of the topology matrix. Blind estimation of states and the real-value topology has been studied in [13]. However, all these methods estimate the real-valued susceptance matrix and are based on using *linearized* power flow models (i.e. the DC model). Other methods include data-driven approaches using the historical smart meter measurements [14], an active sensing of grid probing of voltage data [15], and graphical models for topology learning [16], [17]. However, model-based estimation of the complex-valued admittance matrix under Laplacian constraints based on the AC model has not been done before.

In this paper, we investigate the estimation of the admittance matrix, including the topological information (connectivity pattern) and line parameters (weights), based on phasor measurements of voltage and power data. The system admittance matrix is a complex symmetric matrix, whose real and (minus) imaginary parts are real-valued Laplacian matrices. We assume the nonlinear AC model of the power flow and formulate the associated constrained maximum likelihood (CML) estimator under the Laplacian and sparsity constraints. This estimation can be interpreted as a graph learning problem with the unique characteristics of the electrical network. In order to implement the CML estimator efficiently, we develop the associated alternating direction method of multipliers (ADMM) algorithm [18]. Simulations demonstrate that the proposed ADMM algorithm outperforms existing methods for the IEEE 14-bus test case.

In the rest of this paper vectors are denoted by boldface lowercase letters and matrices by boldface uppercase letters. The $K \times K$ identity matrix is denoted by $\mathbf{I}_K$, and $\mathbf{1}$ and $\mathbf{0}$ denote the vectors of ones and zeros. The notations $|\cdot|$, $\otimes$, and $\odot$, denote the determinant operator, and the Kronecker and the Hadamard products, respectively. For any vector $\mathbf{u}$, $\|\mathbf{u}\|_2$ denotes the Euclidean-norm. For any matrix $\mathbf{A}$, $\mathbf{A} \succeq \mathbf{0}$ implies that $\mathbf{A}$ is a positive semi-definite matrix, $\mathbf{A}^{-1}$ and $\|\mathbf{A}\|_F$ are its inverse and Frobenius norm, respectively, $\|\mathbf{A}\|_{1,\text{off}}$ is the sum of absolute values of all off-diagonal elements of $\mathbf{A}$, and $\text{vec}(\mathbf{A})$ is the vector obtained by stacking the columns of $\mathbf{A}$ with $\text{unvec}(\text{vec}(\mathbf{A})) = \mathbf{A}$. For a vector $\mathbf{a}$, $\text{diag}(\mathbf{a})$ is a diagonal matrix whose ith diagonal entry is $\mathbf{a}_i$, $x^+ = \max\{x, 0\}$, and $\text{Soft}(x, a) \triangleq \text{sign}(x)\{|x| - a\}^+$.

II. MODEL AND PROBLEM FORMULATION

In this paper, we consider the problem of estimating the admittance matrix in electrical networks by exploiting phasor measurements of voltages and power data. In this section, we present the power network as a graph, describe the measurement model, and formulate the estimation problem.

A power system can be represented as an undirected connected weighted graph, $\mathcal{G}(\mathcal{V},\xi)$, where the set of vertices, $\mathcal{V}=\{1,\ldots,M\}$, includes the buses (generators/loads) and the set of edges, ξ, includes the transmission lines. The edge $(m,k)\in\xi$ corresponds to the transmission line between buses m and k and is characterized by the line admittance, $y_{m,k}\in\mathbb{C}$. The system (nodal) admittance matrix is a $M\times M$ complex matrix, where its (m,k) element is (p. 97 in [19])

$$[\mathbf{Y}]_{m,k}=\begin{cases}-\sum\limits_{n\in\mathcal{N}_m} y_{m,n}, & m=k\\ y_{m,k}, & m\neq k\\ 0, & \text{otherwise}\end{cases}, \tag{1}$$

$\forall(m,k)\in\xi$. In this graph representation, the admittance matrix from (1) can be decomposed as follows:

$$\mathbf{Y}=\mathbf{G}+j\mathbf{B}, \tag{2}$$

where the conductance matrix, $\mathbf{G}\in\mathbb{R}^{M\times M}$, and the minus of the susceptance matrix, $\tilde{\mathbf{B}}\stackrel{\triangle}{=}-\mathbf{B}\in\mathbb{R}^{M\times M}$, are both real Laplacian matrices. In addition, in conventional electrical networks these matrices are sparse. Thus, the matrices $\mathbf{G}$ and $\tilde{\mathbf{B}}$ have the following properties [1]:

P.1) symmetry: $\mathbf{G}=\mathbf{G}^T$, $\tilde{\mathbf{B}}=\tilde{\mathbf{B}}^T$
P.2) null-space property: $\mathbf{G}\mathbf{1}=\mathbf{0}$, $\tilde{\mathbf{B}}\mathbf{1}=\mathbf{0}$
P.3) positive semi-definiteness: $\mathbf{G}\succeq\mathbf{0}$, $\tilde{\mathbf{B}}\succeq\mathbf{0}$
P.4) non-positive off-diagonal entries: $[\mathbf{G}]_{m,k}\leq 0$, $[\tilde{\mathbf{B}}]_{m,k}\leq 0$, $\forall m,k=1,\ldots,M$, $m\neq k$
P.5) $\mathbf{G}$ and $\tilde{\mathbf{B}}$ are sparse matrices.

As a result, $\mathbf{Y}$ is a symmetric (non-hermitian) matrix.

With this admittance matrix at hand, we consider the commonly-used nonlinear AC power flow model [1], [2]. According to this model, which is based on Kirchhoff's and Ohm's laws, the injected complex power satisfies

$$s_m=v_m\left(\sum\nolimits_{k=1}^{M} y_{m,k}v_k\right)^*,\ m=1,\ldots,M, \tag{3}$$

where s_m and v_m denote the complex power injection and voltage phasors, respectively, at bus m. Therefore, the measurements of M active power injections at the M buses over N time samples and with additional noise, can be written in a matrix form as follows:

$$\mathbf{s}[n]=\text{diag}(\mathbf{v}[n])\mathbf{Y}^*\mathbf{v}[n]^*+\boldsymbol{\eta}[n],\ n=0,\ldots,N-1, \tag{4}$$

where $\mathbf{s}[n]\stackrel{\triangle}{=}[s_1[n],\ldots,s_M[n]]^T$, $\mathbf{v}[n]\stackrel{\triangle}{=}[v_1[n],\ldots,v_M[n]]^T$, and the noise sequence, $\{\boldsymbol{\eta}[n]\}_{n=0}^{N-1}$, is a complex circularly symmetric Gaussian i.i.d. random vector with zero mean and a known covariance matrix $\mathbf{R}_\eta$.

In this paper, we consider the task of recovering the deterministic complex-valued matrix $\mathbf{Y}$, or equivalently, the real-valued matrices $\mathbf{G}$ and $\tilde{\mathbf{B}}$. The power and voltage data are assumed to be known and can be obtained by phasor measurement units (PMUs) [1]. The log-likelihood function of the model in (4) after substituting (2) is [20]:

$$\mathcal{L}(\mathbf{G},\tilde{\mathbf{B}})=-MN\log 2\pi-N\log|\mathbf{R}_\eta|-\psi(\mathbf{G},\tilde{\mathbf{B}}), \tag{5}$$

where

$$\psi(\mathbf{G},\tilde{\mathbf{B}})\stackrel{\triangle}{=}\sum_{n=0}^{N-1}\left\|\mathbf{s}[n]-\text{diag}(\mathbf{v}[n])(\mathbf{G}+j\tilde{\mathbf{B}})\mathbf{v}^*[n]\right\|^2_{\mathbf{R}_\eta^{-1}}. \tag{6}$$

It can be seen that in contrast to Laplacian learning in Gaussian Markov random field models, where the precision (inverse covariance) is usually a *real-valued* Laplacian matrix [21], [22], here we have a physical model, in which the *complex-valued* Laplacian is in the expectation of the measurement model.

III. ADMITTANCE MATRIX ESTIMATION

In this section, we first present the CML estimator of the admittance matrix in Subsection III-A. Since finding the CML estimator is a sparse non-convex optimization problem, we suggest an iterative practical method, the ADMM algorithm [18], to solve this optimization in Subsection III-B.

III-A. Constrained Maximum Likelihood

Based on (5) under the parametric constraints described by properties P.1-P.5 of the Laplacian matrices, $\mathbf{G}$ and $\tilde{\mathbf{B}}$, the CML estimator for $\mathbf{G}$ and $\tilde{\mathbf{B}}$ can be written as the following optimization problem:

$$\begin{aligned}&\min_{\mathbf{G},\tilde{\mathbf{B}}\in\mathbb{R}^{M\times M}}\psi(\mathbf{G},\tilde{\mathbf{B}})\quad\text{such that:}\\ &\text{C.1) }\mathbf{G}=\mathbf{G}^T\ \tilde{\mathbf{B}}=\tilde{\mathbf{B}}^T\\ &\text{C.2) }\mathbf{G}\mathbf{1}=\mathbf{0},\ \tilde{\mathbf{B}}\mathbf{1}=\mathbf{0}\\ &\text{C.3) }[\mathbf{G}]_{m,k}\leq 0,\ [\tilde{\mathbf{B}}]_{m,k}\leq 0,\ \forall m,k=1,\ldots,M,\ m\neq k\\ &\text{C.4) }\mathbf{G}\succeq\mathbf{0},\ \tilde{\mathbf{B}}\succeq\mathbf{0}\\ &\text{C.5) }\mathbf{G},\ \tilde{\mathbf{B}}\text{ are sparse matrices,}\end{aligned} \tag{7}$$

where $\psi(\mathbf{G},\tilde{\mathbf{B}})$ is defined in (6).

First, we note that symmetric, strict diagonally-dominant matrices with real non-negative diagonal entries, such as $\mathbf{G}$ and $\tilde{\mathbf{B}}$ under Constraints C.1-C.3, are necessarily positive semi-definite matrices (see, e.g. p. 392 in [23]). Therefore, Constraint C.4 is redundant and can be removed without changing the solution of (7). In addition, the optimization problem in (7) is a non-convex optimization problem due to the sparsity implied by Constraint C.5. Constraints C.2 and C.3 imply that the diagonal elements of $\mathbf{G}$ and $\tilde{\mathbf{B}}$ are positive. Thus, the sparsity constraint can be approximated by using an ℓ_1 regularization term only on the off-diagonal elements of $\mathbf{G}$ and $\tilde{\mathbf{B}}$ [24]. That is, we remove Constraints C.4 and C.5, and change the objective function in (7) to obtain the following regularized convex optimization problem:

$$\begin{aligned}&\min_{\mathbf{G},\tilde{\mathbf{B}}\in\mathbb{R}^{M\times M}}\psi(\mathbf{G},\tilde{\mathbf{B}})+\lambda\left\|\mathbf{G}\right\|_{1,\text{off}}+\lambda\left\|\tilde{\mathbf{B}}\right\|_{1,\text{off}}\\ &\qquad\text{s.t. C.1)-C.3) are satisfied,}\end{aligned} \tag{8}$$

where $\lambda \in \mathbb{R}^+$ is a regularization parameter. It is well known in the compressed sensing literature that if the unknown matrices are sufficiently sparse, and under some conditions on N and on the model, the minimization in (8) approaches the solution of (7) with overwhelming probability [24].

The problem in (8) without the constraints is the problem of recovering an unknown sparse matrix $\mathbf{Y}$ from the matrix sketch $\mathbf{A}_1\mathbf{Y}\mathbf{A}_2^T$, with known matrices $\mathbf{A}_1$ and $\mathbf{A}_2$. This problem has been extensively studied in different contexts for real matrices $\mathbf{Y}$ [25], [26]. In this work, $\mathbf{Y}$ is a complex matrix, and there are additional linear equality and inequality constraints. Thus, by using the results in [25], [26], it can be shown that the problem in (8) is convex.

III-B. ADMM Algorithm for Topology Identification

The regularized optimization problem in (8), which stems from the CML estimator, can be solved using the ADMM algorithm [18]. The ADMM algorithm utilizes variable splitting, thus introducing two additional auxiliary variables, $\mathbf{Z}_G$ and $\mathbf{Z}_B$, in order to decouple the regularizers from the likelihood term, $\psi(\mathbf{G},\tilde{\mathbf{B}})$, and adds a consistency constraint. The resulting reformulation of (8) is expressed as

$$\min_{\mathbf{G},\tilde{\mathbf{B}},\mathbf{Z}_G,\mathbf{Z}_B\in\mathbb{R}^{M\times M}} \psi(\mathbf{G},\tilde{\mathbf{B}}) + \lambda\left\|\mathbf{Z}_G\right\|_{1,\text{off}} + \lambda\left\|\mathbf{Z}_B\right\|_{1,\text{off}}$$
$$\text{s.t.} \begin{cases} \text{C.0) } \mathbf{Z}_G = \mathbf{G},\ \mathbf{Z}_B = \tilde{\mathbf{B}} \\ \text{C.1)-C.3) are satisfied.} \end{cases} \tag{9}$$

In order to solve (9) by the ADMM algorithm, we formulate the scaled augmented Lagrangian function [18]:

$$\begin{aligned} & L_\rho(\mathbf{G},\tilde{\mathbf{B}},\mathbf{Z}_G,\mathbf{Z}_B,\mathbf{U}_G,\mathbf{U}_B,\boldsymbol{\mu}_G,\boldsymbol{\mu}_B,\mathbf{V}_G,\mathbf{V}_B,\boldsymbol{\Lambda}_G,\boldsymbol{\Lambda}_B) \\ & \triangleq \psi(\mathbf{G},\tilde{\mathbf{B}}) + \lambda\|\mathbf{Z}_G\|_{1,\text{off}} + \lambda\|\mathbf{Z}_B\|_{1,\text{off}} \\ & \quad + K_\rho(\mathbf{G},\mathbf{Z}_G,\mathbf{U}_G,\boldsymbol{\mu}_G,\mathbf{V}_G,\boldsymbol{\Lambda}_G) \\ & \quad + K_\rho(\tilde{\mathbf{B}},\mathbf{Z}_B,\mathbf{U}_B,\boldsymbol{\mu}_B,\mathbf{V}_B,\boldsymbol{\Lambda}_B), \end{aligned} \tag{10}$$

where

$$\begin{aligned} & K_\rho(\mathbf{G},\mathbf{Z}_G,\mathbf{U}_G,\boldsymbol{\mu}_G,\mathbf{V}_G,\boldsymbol{\Lambda}_G) \\ & \quad \triangleq \frac{\rho}{2}(\|\mathbf{G}\mathbf{1}+\rho^{-1}\boldsymbol{\mu}_G\|_2^2 - \|\rho^{-1}\boldsymbol{\mu}_G\|_2^2) \\ & \quad + \frac{\rho}{2}(\|\mathbf{Z}_G-\mathbf{G}+\rho^{-1}\mathbf{U}_G\|_F^2 - \|\rho^{-1}\mathbf{U}_G\|_F^2) \\ & \quad + \frac{\rho}{2}(\|\mathbf{G}-\mathbf{G}^T+\rho^{-1}\mathbf{V}_G\|_F^2 - \|\rho^{-1}\mathbf{V}_G\|_F^2) \\ & \quad + \frac{1}{2\rho}\sum_{m=1}^{M}(\sum_{k=1}^{M}(((\{[\boldsymbol{\Lambda}_G]_{m,k}+\rho[\mathbf{G}]_{m,k}\}^+)^2 - [\boldsymbol{\Lambda}_G]_{m,k}^2)), \end{aligned} \tag{11}$$

and $\mathbf{U}_G$, $\mathbf{U}_B$, $\boldsymbol{\mu}_G$, $\boldsymbol{\mu}_B$, $\mathbf{V}_G$, and $\mathbf{V}_B$ are the scaled Lagrangian multipliers of the equality constraints, and $\boldsymbol{\Lambda}_G$ and $\boldsymbol{\Lambda}_B$ are the multipliers of the inequality constraints, and ρ is an additional optimization variable. Since as problem (8) is convex, the proposed ADMM converges for all $\rho > 0$ under mild conditions. By using the scaled augmented Lagrangian in (10), we can solve (9) in an alternating fashion. This results in the following three-stage ADMM update equations for the ith iteration.

In **Stage 1**, we update the primal variables and their duplicates, as follows:

$$\begin{aligned} & \mathbf{G}^{(i+1)} = \arg\min_{\mathbf{G}\in\mathbb{R}^{M\times M}} L_\rho(\mathbf{G},\tilde{\mathbf{B}}^{(i)},\mathbf{Z}_G^{(i)},\ldots,\boldsymbol{\Lambda}_G^{(i)},\boldsymbol{\Lambda}_B^{(i)}) \\ & = \arg\min_{\mathbf{G}\in\mathbb{R}^{M\times M}} \psi(\mathbf{G},\tilde{\mathbf{B}}) + K_\rho(\mathbf{G},\mathbf{Z}_G^{(i)},\mathbf{U}_G^{(i)},\boldsymbol{\mu}_G^{(i)},\mathbf{V}_G^{(i)},\boldsymbol{\Lambda}_G^{(i)}) \\ & = \text{unvec}\Bigg(\mathbf{Q}(\mathbf{G}^{(i)},\boldsymbol{\Lambda}_G^{(i)},\rho)\,(\text{Re}\{\mathbf{T}_0\} \\ & \qquad + \text{Im}\{\mathbf{T}_1\}\text{vec}(\tilde{\mathbf{B}}^{(i)}) + \text{vec}(\rho\mathbf{Z}_G^{(i)} + \mathbf{U}_G^{(i)} - \boldsymbol{\mu}_G^{(i)}\mathbf{1}^T \\ & \qquad - \mathbf{V}_G^{(i)} + (\mathbf{V}_G^{(i)})^T - \boldsymbol{\Lambda}_G^{(i)}\mathbb{1}_{\{\boldsymbol{\Lambda}_G^{(i)}+\rho\mathbf{G}^{(i)}>0\}})\Bigg) \end{aligned} \tag{12}$$

$$\begin{aligned} & \tilde{\mathbf{B}}^{(i+1)} = \arg\min_{\tilde{\mathbf{B}}\in\mathbb{R}^{M\times M}} L_\rho(\mathbf{G}^{(i+1)},\tilde{\mathbf{B}},\mathbf{Z}_G^{(i)},\ldots,\boldsymbol{\Lambda}_G^{(i)},\boldsymbol{\Lambda}_B^{(i)}) \\ & = \arg\min_{\tilde{\mathbf{B}}\in\mathbb{R}^{M\times M}} \psi(\mathbf{G},\tilde{\mathbf{B}}) + K_\rho(\tilde{\mathbf{B}},\mathbf{Z}_B^{(i)},\mathbf{U}_B^{(i)},\boldsymbol{\mu}_B^{(i)},\mathbf{V}_B^{(i)},\boldsymbol{\Lambda}_B^{(i)}) \\ & = \text{unvec}\Bigg(\mathbf{Q}(\tilde{\mathbf{B}}^{(i)},\boldsymbol{\Lambda}_B^{(i)},\rho)\,(-\text{Im}\{\mathbf{T}_0\} \\ & \qquad - \text{Im}\{\mathbf{T}_1\}\text{vec}(\mathbf{G}^{(i+1)}) + \text{vec}(\rho\mathbf{Z}_B^{(i)} + \mathbf{U}_B^{(i)} - \boldsymbol{\mu}_B^{(i)}\mathbf{1}^T \\ & \qquad - \mathbf{V}_B^{(i)} + (\mathbf{V}_B^{(i)})^T - \boldsymbol{\Lambda}_B^{(i)}\mathbb{1}_{\{\boldsymbol{\Lambda}_B^{(i)}+\rho\tilde{\mathbf{B}}^{(i)}>0\}})\Bigg), \end{aligned} \tag{13}$$

where the data-based terms are

$$\mathbf{T}_0 \triangleq 2\sum_{n=0}^{N-1} \text{vec}\left(\text{diag}(\mathbf{v}[n])\mathbf{R}_\eta^{-1}\mathbf{s}^*[n]\mathbf{v}^H[n]\right),$$

$$\mathbf{T}_1 \triangleq 2\sum_{n=0}^{N-1}(\mathbf{v}[n]\mathbf{v}^H[n])\otimes(\text{diag}(\mathbf{v}^H[n])\mathbf{R}_\eta^{-1}\text{diag}(\mathbf{v}[n])),$$

and, for any arbitrary matrices $\mathbf{A}_1$ and $\mathbf{A}_2$, we have

$$\begin{aligned} & \mathbf{Q}(\mathbf{A}_1,\mathbf{A}_2,\rho) \triangleq \Bigg(\text{Re}\{\mathbf{T}_1\} + \rho(3+\mathbb{1}_{\{\mathbf{A}_2+\rho\mathbf{A}_1>0\}})\mathbf{I}_{M^2} \\ & \qquad + \rho\mathbf{1}\mathbf{1}^T\otimes\mathbf{I}_M - 2\rho\sum_{i=1}^{M}\sum_{j=1}^{M}(\mathbf{e}_i\mathbf{e}_j^T)\otimes(\mathbf{e}_j\mathbf{e}_i^T)\Bigg)^{-1}. \end{aligned} \tag{14}$$

In **Stage 2**, the z-minimization step, is obtained by minimizing L_ρ from (10) w.r.t $\mathbf{Z}_G$ and $\mathbf{Z}_B$, after updating the matrices $\mathbf{G}$ and $\mathbf{B}$ to the $i+1$ iteration, i.e. to $\mathbf{G}^{(i+1)}$ and $\tilde{\mathbf{B}}^{(i+1)}$. This minimization results in

$$[\mathbf{Z}_G^{(i+1)}]_{m,k} \triangleq \text{Soft}\left([\mathbf{G}^{(i+1)} - \rho^{-1}\mathbf{U}_G^{(i)}]_{m,k}, \frac{\lambda}{\rho}\right) \tag{15}$$

$$[\mathbf{Z}_B^{(i+1)}]_{m,k} \triangleq \text{Soft}\left([\tilde{\mathbf{B}}^{(i+1)} - \rho^{-1}\mathbf{U}_B^{(i)}]_{m,k}, \frac{\lambda}{\rho}\right), \tag{16}$$

$\forall m \neq k = 1,\ldots,M$.

In **Stage 3**, we update the Lagrangian multipliers as follows:

$$\begin{aligned} \mathbf{U}_G^{(i+1)} &= \mathbf{U}_G^{(i)} + \rho\left(\mathbf{Z}_G^{(i+1)} - \mathbf{G}^{(i+1)}\right) \\ \mathbf{U}_B^{(i+1)} &= \mathbf{U}_B^{(i)} + \rho\left(\mathbf{Z}_B^{(i+1)} - \tilde{\mathbf{B}}^{(i+1)}\right) \\ \boldsymbol{\mu}_G^{(i+1)} &= \boldsymbol{\mu}_G^{(i)} + \rho\left(\mathbf{G}^{(i+1)}\mathbf{1}\right) \\ \boldsymbol{\mu}_B^{(i+1)} &= \boldsymbol{\mu}_B^{(i)} + \rho\left(\tilde{\mathbf{B}}^{(i+1)}\mathbf{1}\right) \end{aligned} \tag{17}$$

$$
\begin{aligned}
\mathbf{V}_G^{(i+1)} &= \mathbf{V}_G^{(i)} + \rho\left(\mathbf{G}^{(i+1)} - (\mathbf{G}^{(i+1)})^T\right) \\
\mathbf{V}_B^{(i+1)} &= \mathbf{V}_B^{(i)} + \rho\left(\tilde{\mathbf{B}}^{(i+1)} - (\tilde{\mathbf{B}}^{(i+1)})^T\right) \\
\mathbf{\Lambda}_G^{(i+1)} &= \left\{\mathbf{\Lambda}_G^{(i)} + \rho\mathbf{G}^{(i+1)}\right\}^+ \\
\mathbf{\Lambda}_B^{(i+1)} &= \left\{\mathbf{\Lambda}_B^{(i)} + \rho\tilde{\mathbf{B}}^{(i+1)}\right\}^+ .
\end{aligned} \tag{18}
$$

After the algorithm converges, we threshold the off-diagonal elements of the matrices $\mathbf{G}$ and $\mathbf{B}$, where the threshold value was set by trial and error.

IV. SIMULATIONS

In this section, we illustrate the performance of recovering the admittance matrix by the ADMM algorithm from Subsection III-B. We use the IEEE 14-Bus test case, which is commonly used in power systems, with the parameters from [27]. The voltages were randomly generated with a uniform distribution in the interval $[0, 1]$. All simulations are averaged over 100 Monte-Carlo simulations for each scenario.

In the implementation of the ADMM algorithm, we initialized the Laplacian matrices, $\mathbf{G}^{(0)}$ and $\tilde{\mathbf{B}}^{(0)}$, by the real and imaginary parts of the sample covariance matrices after removing the positive off-diagonal elements of these matrices and changing the diagonal elements such that Constrained C.2 is satisfied. Then, we initialize the primal parameters to $\mathbf{Z}_G^{(0)} = \mathbf{G}^{(0)}$, $\mathbf{Z}_B^{(0)} = \tilde{\mathbf{B}}^{(0)}$ and the Lagrange multipliers were set to $\mathbf{0}$. The stopping rule was set to $\|\mathbf{G}^{(k+1)} - \mathbf{G}^{(k)}\| < \epsilon$ and $\|\tilde{\mathbf{B}}^{(k+1)} - \tilde{\mathbf{B}}^{(k)}\| < \epsilon$. Finally, the choice of the parameter ρ in general ADMM algorithms is often an involved task [28]. Here we use $\rho = 0.1$.

We compare the performance of the proposed ADMM algorithm with the following methods: 1) The block coordinate descent (BCD) method in [9] with the regularizer $\mu = 14$ and the step size $\beta = 10^{-4}$; and 2) The ADMM algorithm for the DC model in [10], with the penalty $\rho = 0.0001$ and the regularizer $\lambda = 5$. These two methods jointly estimate $\tilde{\mathbf{B}}$ and the angle of $\mathbf{v}[n]$ based on the DC model, which is a linearization of the model in (4) with measurements of the real power injections ($\text{Re}\{\mathbf{s}[n]\}$). In order to have a fair comparison, we insert $\mathbf{v}[n]$ as an input to these methods.

In Fig. 1a, we present the MSE of the different estimators of $\tilde{\mathbf{B}}$ and of the proposed estimator of $\mathbf{G}$ versus the signal-to-noise ratio (SNR), SNR $= 10\log(\frac{1}{MN\sigma^2}\sum_{n=0}^{N-1}\|\mathbf{s}[n]\|^2)$ for $N = 400$. In Fig. 1b we present the F-score metric [21], which measures the classification error probability in the connectivity of the matrices $\tilde{\mathbf{B}}$ and $\mathbf{G}$, i.e. in the sparsity pattern. The F-score takes values between 0 and 1, where the value 1 means perfect classification. It can be seen that the proposed ADMM algorithm, developed for the non-linear model in (4), outperforms the BCD and the ADMM-CD methods, that assume the linearized DC model, in both terms of MSE and F-score for estimating $\tilde{\mathbf{B}}$. This result demonstrates the value of using a more accurate description of the power flow model, i.e. the use of the AC model in (4) versus the use of the DC model by the other methods. In addition, the ADMM algorithm uses phasor measurements obtained by PMUs and a complex-valued admittance that yield a more accurate description of the topology. It can be seen also that the DC-ADMM method in [10] achieves better results than the BCD method in [9]. From a computational complexity point of view, the two methods [9], [10] require using eigenvalue decomposition at each iteration, which is costly as the number of nodes increases. It is interesting to note that for the proposed ADMM algorithm, the F-score performance of the matrix $\tilde{\mathbf{B}}$ is lower than those of the $\mathbf{G}$. This result can be improved by adding a constraint on the connectivity pattern of $\mathbf{G}$ and $\tilde{\mathbf{B}}$, since in general power systems, the sparsity pattern of these matrices is very similar.

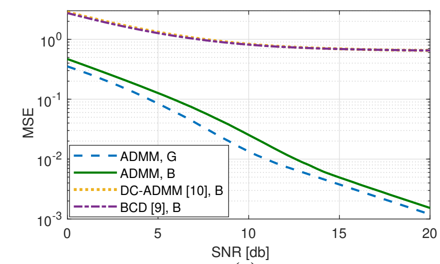

(a)

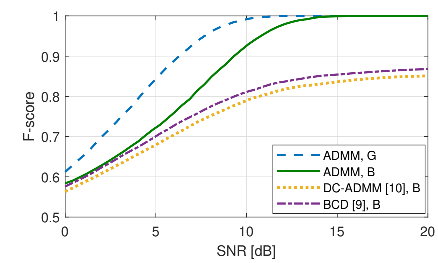

(b)

Fig. 1: The MSE (a) and F-score (b) of the different estimators of the admittance matrix for IEEE 14-bus system.

V. CONCLUSION

Recovering the admittance matrix in power systems plays an essential role in line aging detection, controlling the system operation, planning, and verification during the process of the power system. In this paper, we introduce the CML estimator and its implementation by the ADMM algorithm for estimating the complex-valued admittance matrix of the power grid. This estimation can be interpreted as a complex Laplacian learning under a physical model. The results show that the proposed method achieves better performance than previous methods that use the simplified DC model. In future research, we aim to include also blind scenarios, in which some of the voltage measurements are missing and should be estimated as well. In addition, the development of graph signal processing (GSP) tools for complex-valued Laplacian matrix, which is a symmetric non-hermitian matrix, is of great importance for various applications in power systems.

VI. ACKNOWLEDGMENT

This research was supported by the Israel Ministry of Infrastructure, Energy, and Water Resources and by the BGU Cyber Security Research Center.

VII. REFERENCES

[1] A. Abur and A. Gomez-Exposito, *Power System State Estimation: Theory and Implementation*, Marcel Dekker, 2004.

[2] G. B. Giannakis, V. Kekatos, N. Gatsis, S. J. Kim, H. Zhu, and B. F. Wollenberg, "Monitoring and optimization for power grids: A signal processing perspective," *IEEE Signal Processing Magazine*, vol. 30, no. 5, pp. 107–128, Sept. 2013.

[3] S. Cui, Z. Han, S. Kar, T. T. Kim, H. V. Poor, and A. Tajer, "Coordinated data-injection attack and detection in the smart grid: A detailed look at enriching detection solutions," *IEEE Signal Processing Magazine*, vol. 29, no. 5, pp. 106–115, Sept. 2012.

[4] S. Shaked and T. Routtenberg, "Identification of edge disconnections in networks based on graph filter outputs," *IEEE Trans. Signal and Information Processing over Networks*, vol. 7, pp. 578–594, 2021.

[5] G. Morgenstern and T. Routtenberg, "Structural-constrained methods for the identification of unobservable false data injection attacks in power systems," *arXiv preprint arXiv:2003.08715*, 2021.

[6] E. Drayer and T. Routtenberg, "Detection of false data injection attacks in smart grids based on graph signal processing," *IEEE Systems Journal*, vol. 14, no. 2, pp. 1886–1896, 2020.

[7] R. Emami and A. Abur, "Tracking changes in the external network model," in *North American Power Symposium 2010*, Sep. 2010, pp. 1–6.

[8] Y. Sharon, A. M. Annaswamy, A. L. Motto, and A. Chakraborty, "Topology identification in distribution network with limited measurements," in *PES Innovative Smart Grid Technologies (ISGT)*, Jan. 2012, pp. 1–6.

[9] X. Li, H. V. Poor, and A. Scaglione, "Blind topology identification for power systems," in *IEEE International Conference on Smart Grid Communications (SmartGridComm)*, Oct. 2013, pp. 91–96.

[10] A. Anwar, A. Mahmood, and M. Pickering, "Estimation of smart grid topology using SCADA measurements," in *SmartGridComm*, Nov. 2016, pp. 539–544.

[11] V. Kekatos, G. B. Giannakis, and R. Baldick, "Online energy price matrix factorization for power grid topology tracking," *IEEE Trans. Smart Grid*, vol. 7, no. 3, pp. 1239–1248, May 2016.

[12] S. Xie, J. Yang, K. Xie, Y. Liu, and Z. He, "Low-sparsity unobservable attacks against smart grid: Attack exposure analysis and a data-driven attack scheme," *IEEE Access*, vol. 5, pp. 8183–8193, 2017.

[13] S. Grotas, Y. Yakoby, I. Gera, and T. Routtenberg, "Power systems topology and state estimation by graph blind source separation," *IEEE Trans. Signal Processing*, vol. 67, no. 8, pp. 2036–2051, Apr. 2019.

[14] Y. Liao, Y. Weng, G. Liu, and R. Rajagopal, "Urban MV and LV distribution grid topology estimation via group Lasso," *IEEE Trans. Power Systems*, 2018.

[15] G. Cavraro and V. Kekatos, "Graph algorithms for topology identification using power grid probing," *IEEE Control Systems Letters*, vol. 2, no. 4, pp. 689–694, Oct. 2018.

[16] D. Deka, S. Backhaus, and M. Chertkov, "Structure learning in power distribution networks," *IEEE Trans. Control of Network Systems*, vol. 5, no. 3, pp. 1061–1074, Sept. 2018.

[17] S. Park, D. Deka, and M. Chertkov, "Exact topology and parameter estimation in distribution grids with minimal observability," in *Power Systems Computation Conference (PSCC)*, 2018.

[18] N. Parikh S. Boyd and J. Eckstein E. Chu, B. Peleato, "Distributed optimization and statistical learning via the alternating direction method of multipliers," *IEEE Machine Learning*, vol. 3, no. 1, pp. 1–122, 2011.

[19] A. Monticelli, *State Estimation in Electric Power Systems: A Generalized Approach*, pp. 39–61,91–101,161–199, Springer US, Boston, MA, 1999.

[20] Steven M. Kay, *Fundamentals of statistical signal processing: Estimation Theory*, vol. 1, chapter 7, Prentice Hall PTR, Englewood Cliffs (N.J.), 1993.

[21] H. E. Egilmez, E. Pavez, and A. Ortega, "Graph learning from data under structural and Laplacian constraints," *IEEE Journal of Selected Topics in Signal Processing*, vol. 11, no. 6, pp. 825–841, Sept. 2017.

[22] J. Ying, J. M. Cardoso, and D. Palomar, "Minimax estimation of Laplacian constrained precision matrices," in *International Conference on Artificial Intelligence and Statistics*. PMLR, 2021, pp. 3736–3744.

[23] R. A. Horn and C. R. Johnson, *Matrix Analysis*, Cambridge University Press, New York, NY, USA, 2nd edition, 2012.

[24] M. Elad, *Sparse and redundant representations: from theory to applications in signal and image processing*, vol. 2, New York: Springer Science & Business Media, 2010.

[25] T. Wimalajeewa, Y. C. Eldar, and P. K. Varshney, "Recovery of sparse matrices via matrix sketching," *arXiv preprint arXiv:1311.2448*, 2013.

[26] Y. Rivenson and A. Stern, "Compressed imaging with a separable sensing operator," *IEEE Signal Processing Letters*, vol. 16, no. 6, pp. 449–452, 2009.

[27] "Power systems test case archive," Available: http://www.ee.washington.edu/research/pstca/.

[28] L. Zhao, Y. Wang, S. Kumar, and D. P. Palomar, "Optimization algorithms for graph Laplacian estimation via ADMM and MM," *IEEE Trans. Signal Processing*, vol. 67, no. 16, pp. 4231–4244, 2019.